J. Phys. Chem. A **2009,** *113,* 7267–7274

Theoretical Calculation of Separation Factors for Boron Isotopic Exchange between BF_3 and $BF_3 \cdot C_6H_5OCH_3$[†]

Tao Lin,[‡,§] Weijiang Zhang,[‡] and Lichang Wang*[,§]

School of Chemical Engineering and Technology, Tianjin University, Tianjin 300072, China, and Department of Chemistry and Biochemistry, Southern Illinois University, Carbondale, Illinois 62901

Received: November 24, 2008; Revised Manuscript Received: December 16, 2008

The separation factors (or equilibrium constants) for boron isotopic exchange reaction $^{10}BF_3 + {}^{11}BF_3 \cdot C_6H_5OCH_3 \rightleftarrows {}^{11}BF_3 + {}^{10}BF_3 \cdot C_6H_5OCH_3$ were obtained from MP2/6-31+G(d,p) and B3LYP/6-31+G(d,p) calculations. New scaling factors, single and multiple, were derived from the harmonic frequencies through the least-squares fit for BF_3 and $C_6H_5OCH_3$. The use of multiple scaling factors in the case of $C_6H_5OCH_3$ led to significant improvement in the calculated frequencies over using a single scaling factor. There exists a negligible difference in the separation factors obtained by using the harmonic and the scaled frequencies of the same method, and in those obtained by using different methods. The calculated separation factors for the boron isotopic exchange reaction at 273.15, 293.15, and 298.15K are 1.039, 1.036, and 1.035, respectively, which are in excellent agreement with the experimental values, 1.041 ± 0.002, 1.030 ± 0.002, and 1.035 ± 0.003. This study demonstrated the promise of using DFT (B3LYP) to obtain separation factors for the reactions where the interactions are weaker than covalent bonds but stronger than van der Waals interactions, and consequently to search for better complexation agents than $C_6H_5OCH_3$ for the isotopic separation of BF_3.

1. Introduction

Boron has two stable isotopes, ^{10}B and ^{11}B, with a natural concentration of 19.9% and 80.1%, respectively.[1] Because of the superior ability of ^{10}B in absorbing neutrons (3.837×10^{-25} m^2) compared to that of ^{11}B ($<0.05 \times 10^{-28}$ m^2), great efforts have been devoted to extract ^{10}B from the natural mixture of boron isotopes. Different donor molecules have been studied for their efficiency and practicality in the isotopic exchange reaction, $^{10}BF_3$ (g) + $^{11}BF_3 \cdot$donor (l) $\rightleftarrows$ $^{11}BF_3$ (g) + $^{10}BF_3 \cdot$donor (l). It has been found that oxygen-containing ethers, such as dimethyl ether [DME, $O(CH_3)_2$], diethyl ether [DEE, $O(C_2H_5)_2$], and methylphenyl ether [anisole, $C_6H_5OCH_3$],[2–4] are better donors than thioethers and N-containing compounds that are either toxic, corrosive, unstable, or have a small equilibrium constant (also denoted as separation factor).[5] Anisole has been found so far to be the best donor molecule (or complexation agent) in the $BF_3 \cdot$donor complexes because its use allows the exchange column, where the chemical exchange reaction takes place, to be operated at room temperature and ambient pressure, particularly for its small HETP (the Height Equivalent to a Theoretical Plate).[5–7]

Small HETP can greatly improve column performance but requires a large separation factor for the exchange reaction. To further improve the efficiency and performance of the boron isotopic exchange column, it is essential to obtain separation factors for the exchange reactions of interest. In this work, we investigated the feasibility of using computations to obtain separation factors involving BF_3.

Separation factors for isotopic exchange reactions have been calculated by using vibrational frequencies, which was first employed by Urey and Rittenberg.[8,9] The separation factors of $BF_3 \cdot O(CH_3)_2$ and $BF_3 \cdot O(C_2H_5)_2$ systems were obtained by using frequencies measured by infrared (IR) spectra.[10,11] These separation factors are slightly higher than the experimental values. There are a number of studies on the separation factors that use the calculated vibrational frequencies including $^{34/32}S$,[12] $^{37/35}Cl$,[13] $^{53/52}Cr$,[14] $^{56/54}Fe$,[15,16] $^{97/95}Mo$,[17] and $^{13/12}C$,[18] as well as $^{11/10}B$, in which the exchange reaction takes place between $^{10}B(OH)_3$ and $^{11}B(OH)_4^-$.[19,20] In general, the calculated separation factors are in agreement with the experimental values. However, disagreement is also found in some cases. For instance, the calculated separation factor for $^{10}B(OH)_3$ and $^{11}B(OH)_4^-$ from ab initio molecular dynamics simulations is 0.86, which is very different from the experimental value of 1.028. As such, it is necessary to examine $BF_3 \cdot$donor systems for which experimental separation factors are available before predicting separation factors for other donor molecules that are potential candidates for better exchange column performance.

In this work, we chose $BF_3 \cdot C_6H_5OCH_3$ to investigate whether MP2 (the second-order Møller−Plesset theory) and B3LYP (the Becke's three-parameter exchange functional with the Lee−Yang−Parr correlation functional) methods can be used to obtain the separation factor accurately for the boron isotopic exchange reaction. MP2 and B3LYP calculations were performed to obtain frequencies for the BF_3, $C_6H_5OCH_3$, and $BF_3 \cdot C_6H_5OCH_3$ complex. As the structures of BF_3 and $C_6H_5OCH_3$ are well-known, Figure 1 only shows the most stable structure of the $BF_3 \cdot C_6H_5OCH_3$ complexes,[21] which was used in this work to perform frequency calculations. Harmonic frequencies obtained from ab initio calculations were often larger than the experimental fundamentals. The errors arise from anharmonicity and incomplete treatment of electron correlation.[22] Herein, we chose to use the scaling factor technique to obtain the fundamental frequencies since its use can correct both errors while anharmonic calculations correct only one of the errors.

[†] Part of the "Robert Benny Gerber Festschrift".

* To whom correspondence should be addressed. E-mail: lwang@chem.siu.edu. Phone: (618)4536476.

[‡] Tianjin University.

[§] Southern Illinois University.

10.1021/jp810328r CCC: \$40.75

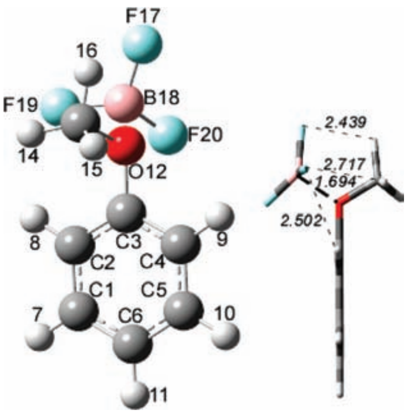

Figure 1. The structure of $BF_3 \cdot C_6H_5OCH_3$ complex obtained from MP2/6-31+G(d,p) calculation. It is denoted as AB13 in ref 21.

A number of studies were devoted to deriving scaling factors. For example, a general study of scaling factors for 19 different levels of theory was conducted by Scott et al.[22] They obtained scaling factors using the least-squares fit to harmonic frequencies as 0.9614 for the B3LYP/6-31G(d) method and 0.9427 for the MP2/6-31G(d,p) method. Additionally, they found that the scaling factor for low-frequency vibrations is not the same as the standard value for the particular method when the evaluation for thermochemical quantities is dominated by low frequencies. Rauhut and Pulay also found that the use of multiple scale factors leads to further significant improvement.[23] Harris conducted a systematic theoretical study of harmonic vibarational frequencies using MP and restricted Hartree−Fock theories and found that ideally isotope effects should be computed from scaled MP2 frequencies with 6-311G(d,p) or 6-311+G(d,p) basis set or a basis set of similar quality.[24] More recently, Irikura et al. reported the uncertainties in scaling factors as 0.9632 ± 0.0211 for B3LYP/6-31+G(d,p) and 0.9398 ± 0.0285 for MP2/6-31+G(d,p).[25] Merrick et al. investigated the effect of basis sets on MP2 and B3LYP scaling factors using basis sets ranging from 6-31G(d) up to 6-311+G(3df,3pd) and obtained the scaling factors 0.9648 for B3LYP/6-31+G(d,p) and 0.9418 for MP2/6-31+G(d,p), respectively,[26] which are in the range of the results of Irikura et al.[25]

In this work, we derived scaling factors from the MP2 and B3LYP harmonic frequencies using the least-squares fit to the experimental fundamentals. The infrared spectra of gaseous, liquid, and solid isotopic BF_3 were reported and discussed more than 40 years ago,[27−29] while the vibrational spectra of gaseous and liquid anisole first appeared in 1983.[30] Recently, Gellini et al. provided the experimental data and derived anharmonicities and force constants of liquid anisole.[31] The scaled B3LYP/6-311G++(d,p) frequencies for neutral gaseous anisole were compared to the experimental frequencies by Eisenhardt et al. and good agreement was obtained.[32] While there is extensive experimental spectroscopic data for BF_3 and $C_6H_5OCH_3$, there is only one infrared experiment for liquid $BF_3 \cdot C_6H_5OCH_3$ complexes.[33] As such, only scaling factors for BF_3 and $C_6H_5OCH_3$ were obtained.

Using the newly derived scaling factors, we obtained fundamental frequencies for BF_3, $C_6H_5OCH_3$, and $BF_3 \cdot C_6H_5OCH_3$. Note that the scaling factor derived from BF_3 was used to obtain the key fundamentals for $BF_3 \cdot C_6H_5OCH_3$. We used both harmonic and fundamental frequencies to obtain separation factors at different temperatures. These results are summarized in section 3. As there is no previous theoretical calculation of separation factors for the isotopic exchange reaction between BF_3 and $BF_3 \cdot C_6H_5OCH_3$, we made the comparison with the experimental values.[4] The methods and technical details used in our calculations are provided in section 2. Finally, the conclusions are drawn in section 4.

2. Method

In this work, we calculated the separation factor (or equilibrium constant) as a function of temperature for the following exchange reaction:

$$^{10}BF_3\ (g) + {}^{11}BF_3 \cdot C_6H_5OCH_3\ (l) \rightleftarrows {}^{11}BF_3\ (g) + {}^{10}BF_3 \cdot C_6H_5OCH_3\ (l) \quad (R1)$$

According to Urey,[9] the separation factor, α, for reaction R1 is defined as,

$$\alpha = (Q_2/Q_1)_a/(Q_2/Q_1)_b \quad (1)$$

where Q values are the partition functions of the molecules that are calculated from the frequencies. The subscripts a and b represent BF_3 and $BF_3 \cdot C_6H_5OCH_3$, respectively. The subscripts 1 and 2 represent the species consisting of ^{10}B and ^{11}B, respectively.

The partition function ratio Q_2/Q_1 (also denoted as β) in eq 1 is expressed as,

$$\beta = \frac{Q_2}{Q_1} = \prod_i \frac{u_{2i}}{u_{1i}} \frac{e^{-u_{2i}/2}}{1 - e^{-u_{2i}}} \frac{1 - e^{-u_{1i}}}{e^{-u_{1i}/2}} \quad (2)$$

where $u_i = hc\omega_i/kT$, and ω_i is the ith normal vibrational frequency. The variables, h, c, k, and T, are the Planck constant, speed of light, the Boltzmann constant, and temperature, respectively.

We performed MP2[34,35] and B3LYP[36−39] frequency calculations for the species in reaction R1 with 6-31+G(d,p) basis set using Gaussian03.[40] The structures used in the frequency calculations are the optimized structures for the corresponding method. In our calculations, only gas phase frequencies were obtained. Note that the partition function ratio for $BF_3 \cdot C_6H_5OCH_3$, i.e. $\beta_b = (Q_2/Q_1)_b$, should be in the liquid phase. The use of gas phase data in the calculation indicates that we actually obtain the separation factor (denoted as α_2) for the following reaction:

$$^{10}BF_3\ (g) + {}^{11}BF_3 \cdot C_6H_5OCH_3\ (g) \rightleftarrows {}^{11}BF_3\ (g) + {}^{10}BF_3 \cdot C_6H_5OCH_3\ (g) \quad (R2)$$

If we obtain the separation factor, denoted as α_3, for the reaction

$$^{10}BF_3 \cdot C_6H_5OCH_3\ (g) + {}^{11}BF_3 \cdot C_6H_5OCH_3\ (l) \rightleftarrows {}^{11}BF_3 \cdot C_6H_5OCH_3\ (l) + {}^{11}BF_3 \cdot C_6H_5OCH_3\ (g) \quad (R3)$$

we can then derive the separation factor for reaction R1 by

$$\alpha = \alpha_2 \times \alpha_3 \quad (3)$$

where α_2 is calculated by using eq 1 with β_b being the gas-phase vibrational frequencies.

Reaction R3 consists of the liquification (or reverse vaporization) of $^{10}BF_3 \cdot C_6H_5OCH_3$ (g) and vaporization of $^{11}BF_3 \cdot C_6H_5OCH_3$ (l). We expect that the difference in the heat of vaporization between these isotopic complexes is mainly due to the zero-point energy difference with $^{10}BF_3 \cdot C_6H_5OCH_3$ having a slightly larger value. This means that the separation factor of reaction R3 will be slightly smaller than but very close

TABLE 1: Vibrational Frequencies (cm^{-1}) of Gaseous $^{10}BF_3$ and $^{11}BF_3$

	$^{10}BF_3$					$^{11}BF_3$				
	B3LYP/6-31+G(d,p)		MP2/6-31+G(d,p)			B3LYP/6-31+G(d,p)		MP2/6-31+G(d,p)		
assignment	harmonic	scaled	harmonic	scaled	exptl[a]	Harmonic[b]	scaled	Harmonic[b]	scaled	exptl[a]
I (ν_1, sym B−F stretch)	876	878	871	878	888	876	886	871	880	888
II (ν_2, BF_3 out-of-plane bend)	708	730	725	730	718	681	689	696	703	691
III (ν_3(2), antisym B−F stretch)	1493	1506	1495	1506	1505	1440	1457	1442	1455	1454
IV (ν_4(2), BF_3 in-plane bend)	470	476	472	476	482	468	473	471	475	480

[a] Data were taken from ref 27. [b] Data were taken from the Supporting Information in ref 21.

to 1, which will be further justified from our calculations and discussed in section 3.3.

The generic frequency scaling factors, λ, were obtained by

$$\lambda = \sum_{i=1}^{\text{all}} \omega_i \gamma_i \Big/ \sum_{i=1}^{\text{all}} \omega_i^2 \qquad (4)$$

where ω_i and γ_i are the ith experimental fundamental and ith theoretical harmonic frequencies (in cm^{-1}), respectively.[22]

Among the multiple scaling factors, those for the medium to high frequency ranges were obtained by using eq 4. Since the contribution from high frequencies is minimal for the low frequency vibrations, the scaling factor for the low frequency range was obtained by using the inverse frequency scaling factor according to Scott and Radom:[22]

$$\lambda = \sum_{i=1}^{\text{all}} \left(\frac{1}{\omega_i}\right)^2 \Big/ \sum_{i=1}^{\text{all}} \frac{1}{\omega_i \gamma_i} \qquad (5)$$

3. Results

3.1. Harmonic Frequencies. The harmonic frequencies of gaseous $^{10}BF_3$ and $^{11}BF_3$ from B3LYP and MP2 calculations are listed in Table 1 together with experimental data. The infrared spectrum of boron trifluoride was first investigated by Gage and Barker.[41] They observed the isotopic effect in all bands and active fundamental vibration frequencies. Furthermore, the infrared spectra of $^{10}BF_3$ and $^{11}BF_3$ were completed and reexamined.[27,42] As shown in Table 1, the harmonic frequencies from both MP2 and B3LYP calculations of $^{10}BF_3$ and $^{11}BF_3$ disagree with the experimental data by 5−17 cm^{-1}. Noticeably, the calculated MP2 frequencies for the υ_2 mode are larger than the experimental values for both isotopes.

The B−F symmetric stretching frequency (υ_1), which is not infrared active, has no shift from $^{10}BF_3$ to $^{11}BF_3$. The out-of-plane bending band (υ_2) has a 27 cm^{-1} red-shift from B3LYP calculations, which is identical with the observed 27 cm^{-1} shift.[27] The red-shift from MP2 calculations is 29 cm^{-1}. Both B3LYP and MP2 calculations provide a red-shift of 53 cm^{-1} for the B−F antisymmetric frequency (υ_3), which is very close to the experimental value of 51 cm^{-1}. As for the BF_3 in-plane bending mode, the B3LYP calculations give a red-shift of 2 cm^{-1}, which is the same as the experimental value. On the other hand, MP2 calculations give the shift as 1 cm^{-1}. The comparison between the calculated harmonic frequencies and the experimental data for BF_3 isotopes shows the following trends: (1) B3LYP data agree better with the experimental values than MP2 data for absolute frequencies. (2) Both B3LYP and MP2 methods predicted the isotopic frequency shifts accurately. (3) The predicted isotopic zero-point energy (ZPE) difference is 1 cm^{-1}, which indicates that either of these methods will predict the same ZPE difference.

The harmonic frequencies of anisole are provided in Table 2 with the experimental values[30] and previous calculations.[32] As shown in Table 2, most calculated harmonic frequencies (MP2 and B3LYP) are larger than the experimental values.[30] Among 42 frequencies, in all but three (modes 4, 12, and 14) the B3LYP data are closer to the experimental values than those of MP2 data. This discrepancy can be classified into three regions, <1000, 1000−2000, and >3000 cm^{-1}. For B3LYP frequencies, the discrepancy increases from <15 cm^{-1} in the range of <1000 cm^{-1}, to ~52 cm^{-1} in the 1000−2000 cm^{-1} range, and further to >100 cm^{-1} in the range of >3000 cm^{-1}. This trend is not surprising, as the major source of the disagreement can be attributed to the neglect of anharmonicity effects in the theoretical treatment. We expect that the anharmonicity increases with frequency; therefore, a larger discrepancy is expected at higher frequencies. This discrepancy can be corrected by using frequency scaling factors and satisfactory agreement between the scaled theoretical frequencies and the experimental frequencies can be obtained, which will be discussed in the next section. Both comparisons, BF_3 and $C_6H_5OCH_3$, show that one can use either MP2 or B3LYP results to make qualitative comparisons between two isotopic species, though the absolute frequencies can be different. Therefore, we choose MP2 results to make comparisons in the following discussion whenever the results from only one method are chosen.

The harmonic frequencies for the complex $^{10}BF_3{\cdot}C_6H_5OCH_3$ that are different from those of $^{11}BF_3{\cdot}C_6H_5OCH_3$ are summarized in Table 3. The difference in the predicted shift between B3LYP and MP2 methods ranges from 1 to 4 cm^{-1}. Furthermore, the isotopic ZPE difference predicted from B3LYP calculations is 113 cm^{-1}, while that from MP2 calculations is 114 cm^{-1}. This indicates that both methods give the same prediction on isotopic ZPE difference.

Figure 2 depicts how the frequencies are shifted when BF_3 and $C_6H_5OCH_3$ form a complex. Among the infrared active modes, frequency shifts of nine modes can be observed and therefore labeled in Figure 2. We first discuss the case of $^{11}BF_3{\cdot}C_6H_5OCH_3$ complex formation. A red-shift of 93 cm^{-1} (from 696 to 603 cm^{-1}) can be found for the υ_2 mode ($^{11}BF_3$ out-of-plane bending). This red-shift can be attributed to the density of localized electrons on the vacant orbital of the boron atom and thus the polarity of the complex increases. The two degenerate B−F antisymmetric stretching frequencies of boron fluoride, mode υ_3, at 1442 cm^{-1} red-shifts and splits into two peaks at 1230 and 1291 cm^{-1} in complex. In the optimized complex structure, as shown in Figure 1, this shift and split occurs due to the destruction of the molecular BF_3 symmetry where the structure of BF_3 deforms from planar to pyramidal and the methyl group rotates −106°.[21] As such, the lone pair electron of the oxygen atom is localized on the vacant orbital of the boron atom, causing the B−F force constant to increase and the force constant of BF_3 out-of-plane bending to decease.

When the anisole interacts with boron trifluoride forming the complex, the oxygen atom donates electrons to the vacant orbital

TABLE 2: Vibrational Frequencies (cm^{-1}) of Gaseous $C_6H_5OCH_3$

	B3LYP/6-31+G(d,p)		MP2/6-31+G(d,p)			
assignment	harmoni[a]	scaled	harmonic[a]	scaled	exptl[b]	calcd[c]
1 (COC torsion)	94	92	65	70	81.5	90
2 (CH_3 torsion)	209	204	179	193	209	203
3 (COC ip bending)	257	251	248	267	260	250
4 (CH_3 torsion)	274	267	264	284	263	266
5 (CCC twisting)	425	415	303	326	415	412
6 (CCO ip bending + ip ring def.)	446	435	381	410		433
7 (CCC twisting)	518	505	444	478	511	502
8 (ip CCO bending + ip ring def.)	559	545	479	516	553	543
9 (ip ring deformation)	627	612	557	600	618	610
10 (ring torsion)	697	680	624	672	690	669
11 (op CCH bending + ring torsion)	763	744	717	772	752	738
12 (ring−O stretching + ip ring def.)	798	779	794	855	788	777
13 (op CCH bending)	828	808	800	862	819	806
14 (op CCH bending)	894	872	827	891	880	867
15 (op CCH bending)	969	945	879	947	956	941
16 (op CCH bending)	989	965	889	958	975	956
17 (ring bending)	1008	983	1016	971	997	981
18 (ring breathing)	1043	1018	1053	1006	1022	1015
19 (O− CH_3 stretching)	1071	1045	1083	1035	1039	1041
20 (ip CCH bending)	1105	1078	1118	1068	1073	1075
21 (CH_3 rocking)	1171	1142	1186	1133	1143	1138
22 (ip CCH bending)	1180	1151	1198	1145	1151	1147
23 (ip CCH bending)	1197	1168	1216	1162	1169	1165
24 (CH_3 rocking)	1206	1177	1224	1170	1180	1173
25 (ring−O stretching + ip CCH bending)	1284	1253	1301	1243	1253	1248
26 (ip CCH bending + C=C stretching)	1342	1309	1358	1298	1292	1305
27 (C=C stretching + ip CCH bending)	1368	1335	1471	1406	1332	1330
28 (CH_3 sym def.)	1478	1442	1502	1435	1442	1437
29 (C=C stretching + ip CCH bending)	1490	1454	1509	1442	1455	1449
30 (CH_3 asym def.)	1498	1461	1534	1466	1452	1456
31 (CH_3 sym def.)	1511	1474	1549	1480	1464	1469
32 (C=C stretching + ip CCH bending)	1534	1497	1558	1489	1497	1492
33 (C=C stretching)	1633	1593	1655	1581	1588	1542
34 (C=C stretching)	1651	1611	1672	1598	1599	1606
35 (CH_3 sym stretching)	3016	2887	3100	2894	2900	2903
36 (CH_3 asym stretching)	3078	2946	3187	2975	2942	2964
37 (CH_3 asym stretching)	3151	3016	3249	3033	3004	3034
38 (ring C−H stretching)	3181	3045	3254	3038	3026	3063
39 (ring C−H stretching)	3188	3051	3257	3041	3037	3070
40 (ring C−H stretching)	3204	3067	3272	3055	3062	3089
41 (ring C−H stretching)	3212	3074	3279	3061	3092	3093
42 (ring C−H stretching)	3221	3083	3291	3072	3105	3101

[a] Data were taken from the Supporting Information in ref 21. [b] Data were taken from ref 30. [c] Data were taken from ref 32.

TABLE 3: Harmonic Frequencies (cm^{-1}) of $BF_3 \cdot C_6H_5OCH_3$ That Shift upon Isotopic Substitution Obtained from B3LYP and MP2 calculations with the 6-31+G(d,p) Basis Set

	$^{10}BF_3 \cdot C_6H_5OCH_3$		$^{11}BF_3 \cdot C_6H_5OCH_3$	
assignment	B3LYP	MP2	B3LYP[a]	MP2[a]
II (ν_2, BF_3 deformation)	591	612	578	603
B−O stretching	601	635	598	630
I (ν_1, sym B−F stretching)	852	854	848	848
24 (CH_3 rocking)	1237	1259	1235	1257
III (ν_3, antisym B−F stretching)	1283	1277	1239	1230
III (ν_3, antisym B−F stretching)	1335	1336	1288	1291

[a] Data were taken from the Supporting Information in ref 21.

of the boron atom and the fluorine atoms receive back-donation from the hydrogen atoms of the methyl group.[21] As a result, the bond distances of C (of benzene ring)−O and O−C (of CH_3) increase, while the C−H bond distances of the methyl group decrease. As seen in Figure 2, the donation and back-donation also results in the ring−O stretching (mode 25) and O−CH_3 stretching (mode 19) at 1301 and 1083 cm^{-1}, respectively, red-shift to 1189 and 1021 cm^{-1} in the complex with the amount of 112 and 62 cm^{-1}, respectively. Also the frequency of mode 31 (the CH_3 symmetric deformation) at 1549 cm^{-1} in anisole decreases to 1409 cm^{-1} in the complex. The C=C stretching at 1672 cm^{-1} of anisole, mode 35, has a red-shift of 16 cm^{-1} as the electrons flow from π electron cloud to the oxygen atom.[21] Two blue-shifts, modes 35 and 36, are observed in Figure 2. These modes correspond to the CH_3 symmetrical and asymmetrical stretching. In free anisole, the force constants of the localized C−H stretching modes, one equatorial (C−H16, see Figure 1) and two axial (C−H14 and C−H15), were calculated to be 5.325 and 5.062 mdyn/Å, respectively.[31] Mckean believed that the lengthening of the axial C−H bonds (C−H14 and C−H15), leading to smaller force constants than the equatorial case, is related to the electron back-donation from the lone pairs of the oxygen atom to the σ^* orbitals of the adjacent C−H bonds.[43] Upon the complex formation, however, we found that the axial bond distances (C−H14 and C−H15) decreased significantly compared to the equatorial C−H bond. As such, these three bond distances become close to one another. This leads to the three force constants of the methyl C−H stretching modes being similar due to the electron back-donation from the fluorine atoms to the axial hydrogen atom (H14 and H15).

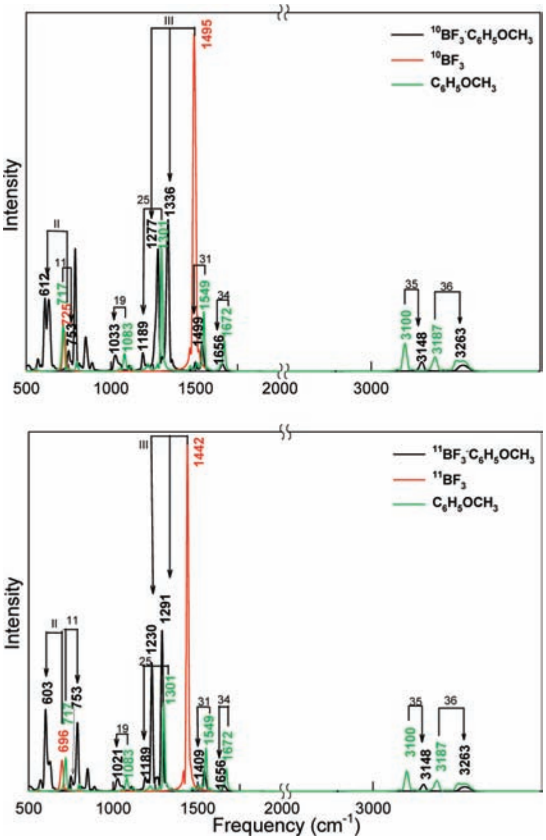

Figure 2. Infrared spectra of gaseous isotopic $BF_3{\cdot}C_6H_5OCH_3$, BF_3, and $C_6H_5OCH_3$ that were obtained from MP2/6-31+G(d,p) calculations.

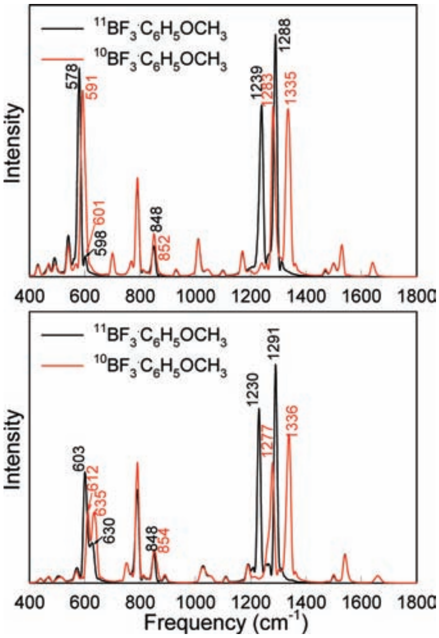

Figure 3. Infrared spectra of $^{10}BF_3{\cdot}C_6H_5OCH_3$ and $^{11}BF_3{\cdot}C_6H_5OCH_3$ that were obtained from B3LYP/6-31+G(d,p) (top) and MP2/6-31+G(d,p) (bottom) calculations.

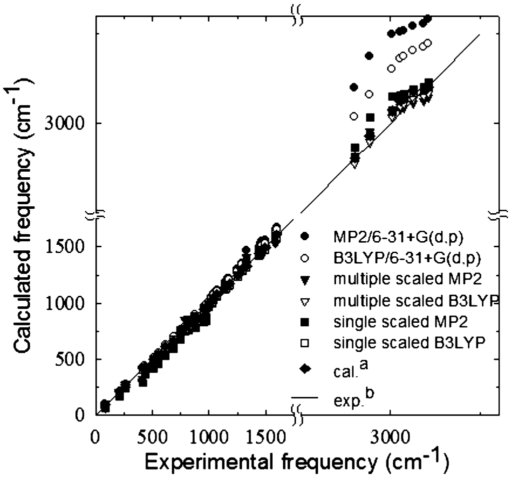

Figure 4. Calculated vibrational frequencies of $C_6H_5OCH_3$ in comparison with the previous theoretical[32] and experimental[30] data.

TABLE 4: Single and Multiple Scaling Factors for $^{10}BF_3$, $^{11}BF_3$, and $C_6H_5OCH_3$

	$C_6H_5OCH_3$		$^{10}BF_3$		$^{11}BF_3$	
	B3LYP	MP2	B3LYP	MP2	B3LYP	MP2
single scale factor	0.9631	0.9460	1.0107	1.0077	1.0123	1.0096
~1000 cm^{-1}	0.9756	1.0769				
1000−2000 cm^{-1}	0.9571	0.9555				
above 2000 cm^{-1}	0.9571	0.9336				

Additionally, with the rotation of the methoxy group, the hydrogen atom in the ortho position (H8) is further apart from the axial hydrogen atoms (H14 and H15) with respect to the van der Waals' radii of hydrogen atoms (2.40 Å), as the closer distance (H8−H14) between the two, is 2.60 Å. We expect that the anharmonicity of C−H8 stretching would increase and be close to the anharmonicities of methyl C−H stretching, 55.1 cm^{-1}.[31]

We now compare the frequency shifts in the boron 10 complex shown in Figure 2. Among 9 infrared active shifts, 5 of them, modes 11, 25, and 34−36, remain the same, as in the case of the boron 11 complex. Four modes, II, III, 19, and 31, shift different amounts of wavenumbers (cm^{-1}) with respect to the boron 11 complex. Furthermore, the frequency shifts of mode III (two of them, ~1230 and 1290 cm^{-1}) are significantly larger than the rest, which is illustrated clearly in Figure 3. Five of the six shifts listed in Table 3 can be found in the infrared spectra in Figure 3. The shift of mode 24, which is about 2 cm^{-1}, cannot be found in Figure 3 due to its negligible intensity. We expect that the separation factor depends mostly on the boron isotopic shift of the BF_3 out-of-plane bending frequencies.

3.2. Scaling Factors and Fundamental Frequencies. The disagreement between the calculated harmonic frequencies and the experimental values shown in Tables 1−3 can be attributed to the neglect of anharmonicity effect and the incomplete treatment of electron correlation. This discrepancy can be corrected by using scaling factors, and thus satisfactory agreement can be achieved between the scaled theoretical and the experimental frequencies. According to the work of Irikura et al., the harmonic frequencies can be scaled by a factor of 0.9398 ± 0.0285 for the MP2/6-31+G(d,p) method with a frozen core approximation and 0.9632 ± 0.0211 for the B3LYP/6-31+G(d) method.[25] Merrick et al. reported a scaling factor of 0.9418 for teh MP2/6-31+G(d,p) method and of 0.9648 for the B3LYP/6-31+G(d,p) method.[26] Eisenhardt et al. found that a better fit to the experimental frequencies for anisole can be achieved by employing multiple scaling factors, in which the scaling factor of 0.973 was used for frequencies in the range up to 2000 cm^{-1} and that of 0.963 was used for those in the range above 2000 cm^{-1} with the B3LYP/6-311+G(d,p) method.[31,32]

To obtain accurate frequencies to be used in the calculation of separation factors, we obtained scaling factors for BF_3 and

TABLE 5: Separation Factors (α, α_2) for Boron Isotope Exchange and the Partition Function Ratios for BF_3 [$\beta_a = (Q_2/Q_1)_a$] and for $BF_3 \cdot C_6H_5OCH_3$ [$\beta_b = (Q_2/Q_1)_b$] as a Function of Temperature for the $BF_3-BF_3 \cdot C_6H_5OCH_3$ System

	B3LYP/6-31+G(d,p)			MP2/6-31+G(d,p)				
T (K)	β_a	β_b	α_2	β_a	β_b	α_2	α	α(exptl)[a]
273.15	1.2803	1.2213	1.048	1.2821	1.2227	1.049	1.039	1.041 ± 0.002
288.15	1.2575	1.2033	1.045	1.2592	1.2045	1.045	1.037	1.033 ± 0.002
293.15	1.2506	1.1978	1.044	1.2522	1.1990	1.044	1.036	1.030 ± 0.002
295.15	1.2479	1.1956	1.044	1.2495	1.1968	1.044	1.036	1.035 ± 0.004
298.15	1.2439	1.1925	1.043	1.2455	1.1936	1.044	1.035	1.035 ± 0.003
299.15	1.2426	1.1914	1.043	1.2442	1.1926	1.043	1.035	1.030 ± 0.001
303.15	1.2375	1.1874	1.042	1.2391	1.1885	1.043	1.034	1.028 ± 0.002
323.15	1.2144	1.1689	1.039	1.2158	1.1700	1.039	1.031	
373.15	1.1695	1.1332	1.032	1.2391	1.1706	1.032	1.026	

[a] Date were taken from ref 4.

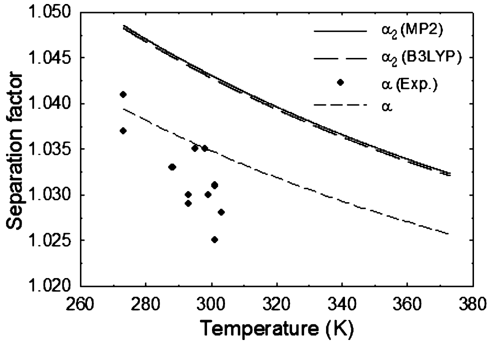

Figure 5. Separation factors (α, α_2) for boron isotopic exchange as a function of temperature for the $BF_3-BF_3 \cdot C_6H_5OCH_3$ system. The experimental data were taken from ref 4.

$C_6H_5OCH_3$. Table 4 summarizes our fitted scaling factors. In Figure 4, we plotted the harmonic and scaled frequencies of $C_6H_5OCH_3$ with the experimental and previous theoretical frequencies. We acquired a single scaling factor of 0.9631 for the entire frequency range for the B3LYP/6-31+G(d,p) method: this value is similar to the 0.9648 obtained by Merrick et al.,[26] and is in the range 0.9632 ± 0.0211 predicted by Irikura et al.[25] Multiple scaling factors of 0.9756 for the frequency range up to 1000 cm^{-1} and of 0.9571 for those above 1000 cm^{-1} were also obtained. It is not surprising that the two factors are reasonably close to one another, as can be seen in Figure 4; the scaled frequencies using a single scaling factor are very similar to the multiple scaled frequencies. Furthermore, both of them give a good approximation to the experimental fundamentals. The challenge in fitting, however, comes from the MP2 harmonic frequencies. There are three frequency regions with different trends compared to the experimental fundamentals. The calculated harmonic frequencies are smaller than the corresponding experimental values in the range up to 1000 cm^{-1}. Then they become larger than the experimental values above 1000 cm^{-1}. More particularly, for the frequencies above 2000 cm^{-1}, they deviate sharply from the experimental frequencies. As such, we obtained three scaling factors, 1.0769, 0.9555, and 0.9336, to correspond to those three parts. Not surprisingly, the single scaled frequencies using the factor of 0.9460 for the MP2/6-31+G(d,p) method (shown in Figure 4, did poorly in fitting the experimental data. Specifically, the single scaled MP2 frequencies at the low frequency range become even more deviated than the corresponding harmonic frequencies with respect to the experimental fundamentals. In summary, the scaled frequencies from our calculations agree rather well with the experimental fundamentals, shown in Figure 4, in which the scaled B3LYP frequencies are still more accurate than the scaled MP2 results in comparison to the experimental fundametals. Multiple scaled frequencies are closer to the fundamentals than the single scaled frequencies. Thus it is acceptable to use multiple scaling factors instead of a single scaling factor. Our results indicate that multiple scaling factors for MP2 frequencies are highly necessary, especially for the compounds that have high frequencies. Upon use of multiple scaling factors, our scaled B3LYP frequencies are more accurate than those calculated by Eisenhardt et al., in which they used a scaling factor of 0.973 in the range 80−2000 cm^{-1} and of 0.963 in the range above 2000 cm^{-1} with the B3LYP/6-311++G(d,p) method.[32]

We obtained the B3LYP/6-31+G(d,p) scaling factor to be 1.0107 for $^{10}BF_3$ and 1.0123 for $^{11}BF_3$ and the MP2/6-31+G(d,p) scaling factor to be 1.0077 for $^{10}BF_3$ and 1.0096 for $^{11}BF_3$.

3.3. Separation Factors. Separation factors for isotopic exchange reactions calculated by using vibrational frequencies were first reported by Urey and Rittenberg.[8,9] Generally, the substitution of a heavy isotope into a substance reduces its vibrational frequencies, leading to a small decrease in vibrational energy. Palko et al. measured the separation factors at various temperatures for the boron isotopic exchange between BF_3 and $BF_3 \cdot O(CH_3)_2$ and compared them with the data obtained from infrared spectral data. A good agreement was found.[10] Jarzecki et al. studied the relationship between the isotopic fractionation factor for the $Fe(H_2O)_6^{3+/2+}$ exchange reaction and the DFT vibrational modes. They obtained the separation factor $\alpha = 1.0054$, contrasting the experimental value $\alpha = 1.0028-1.0030$ at 22 °C.[16,44,45] The authors attributed this disagreement to the use of vibrational spectra on H-bonded crystals, which gave higher Fe−O skeletal frequencies than the ab initio calculations.

Using the scaled vibrational frequencies of $^{10}BF_3$ and $^{11}BF_3$, we obtained the partition function ratio $\beta_a = (Q_2/Q_1)_{BF_3}$ equal to 1.2331 and 1.2311 for the B3LYP and MP2 methods at 298.15 K and ambient pressure, respectively. These results are close to the reported value of 1.2374 at 298.1 K.[9] When we used the harmonic frequencies of $^{10}BF_3$ and $^{11}BF_3$ to calculate the partition function ratio, we obtained the value of 1.2442 from B3LYP/6-31+G(d,p) results and 1.2463 from MP2/6-31+G(d,p) results. With use of the harmonic frequencies shown in Table 3, the calculated partition function ratio value $\beta_b = (Q_2/Q_1)_{BF_3 \cdot C_6H_5OCH_3}$ is 1.1910 and 1.1916 from the B3LYP/6-31+G(d,p) and MP2/6-31+G(d,p) methods, respectively. As there are no experimental frequencies for the gaseous $BF_3 \cdot C_6H_5OCH_3$, we used the scaling factors of $^{10}BF_3$ and $^{11}BF_3$ to obtain the scaled frequencies of $^{10}BF_3 \cdot C_6H_5OCH_3$ and $^{11}BF_3 \cdot C_6H_5OCH_3$. The partition function ratios calculated from the scaled frequencies are 1.1782 and

1.1746 with the B3LYP/6-31+G(d,p) and MP2/6-31+G(d,p) methods, respectively.

Inserting these β values into eq 1, we obtained the separation factors α_2 using harmonic frequencies as 1.045 and 1.046 for the B3LYP/6-31+G(d,p) and MP2/6-31+G(d,p) methods, which are within 1% error with respect to the experimental value $\alpha = 1.035 \pm 0.003$ at 298.15 K.[4] While using the scaled frequencies, we obtained the separation factors as 1.046 and 1.048 from the B3LYP/6-31+G(d,p) and MP2/6-31+G(d,p) methods, respectively. These values are very close to those derived from harmonic frequencies. This is indicative of a negligible difference in separation factors between using harmonic and scaled frequencies, but a substantial difference in partition function ratios. Therefore, the use of harmonic frequencies in the calculation of separation factors is acceptable.

The actual α is even closer to the experimental value as it should be multiplied by another equilibrium constant α_3, which is expected to be slightly smaller than 1. The theoretical calculation of equilibrium constant α_3 is difficult as it requires accurate energy difference of very weak interactions. Here we estimated it by the ratio of experimental α and calculated α_2 at room temperature. This gives $\alpha_3 = 0.9923$. We used this value to derive ΔG for reaction R3 and obtained α_3 at other temperatures. We would also use this value in the future to study new donor molecules that form complexes with BF_3.

Table 5 summarizes the calculated separation factors for both α_2 and α as well as the partition function ratios obtained by using harmonic frequencies at different temperatures. Data in Table 5 show that partition function ratios from B3LYP and MP2 at various temperatures can be different, but the separation factors α_2 are very similar. To make a clear comparison between the calculated and experimental separation factors, we also plotted Figure 5. As shown in Figure 5, the two calculated α_2 values (the solid and long dashed lines) are nearly identical. The short dashed line, representing the separation factor for reaction R1, is among the experimental data at low temperatures, but deviates greatly from the experimental values at higher temperatures. Given the diverse character of the experimental values at high temperatures, we are not sure that this disagreement is entirely due to calculation errors. Further studies from both experimental and theoretical work are clearly needed to resolve this discrepancy.

4. Conclusions

The harmonic frequencies and infrared spectra of isotopic BF_3, $C_6H_5OCH_3$, and isotopic $BF_3 \cdot C_6H_5OCH_3$ complex were obtained by using B3LYP and MP2 methods with the 6-31+G(d,p) basis set. New scaling factors including single and multiple scaling were derived and used to obtain fundamental frequencies. The results show that the use of multiple scaling factors is better in predicting frequencies for molecules having high vibrational frequencies. Separation factors for the isotopic exchange reaction R2 between boron trifluoride and its anisole complex were calculated from vibrational frequencies. Negligible difference was found in the calculated separation factors obtained with the harmonic and the scaled frequencies of the same method and those obtained with different methods. The calculated separation factors for the boron isotopic exchange reaction agree well at temperatures from 273.15 up to 298.15 K. The results demonstrate that B3LYP calculations can be used to obtain separation factors for the reactions involving the interactions that are weaker than covalent bonds but stronger than van der Waals interactions. Furthermore, this study implies that one can use B3LYP calculations to search for better complexation agents than $C_6H_5OCH_3$ for the isotopic separation of BF_3.

Acknowledgment. This work is supported by the Tianjin Science and Technology Project, China (Grant 07ZCKF-GX03900) and the NSF (Grant CBET-0709113). Tao Lin was supported by a fellowship from the China Scholarship Council for his stay at the Southern Illinois University, Carbondale.

References and Notes

(1) Lide, D. R. *CRC Handbook of Chemistry and Physics*, 85 ed.; CRC Press: Boca Raton, FL, 2004; pp 1150.

(2) Palko, A. A. *Ind. Eng. Chem.* **1959**, *51*, 121.

(3) Palko, A. A.; Drury, J. S. *J. Chem. Phys.* **1967**, *46*, 2297.

(4) Palko, A. A.; Healy, R. M.; Landau, L. *J. Chem. Phys.* **1958**, *28*, 214.

(5) Katalnikov, S. G. *Sep. Sci. Technol.* **2001**, *36*, 1737.

(6) Wei, F.; Zhang, W.; Han, M.; Han, L.; Zhang, X.; Zhang, S. *Chem. Eng. Process.* **2008**, *47*, 17.

(7) Han, L.; Yu, J.; Wang, H.; Lin, T.; Zhang, W. *Proc. Int. Forum Green Chem. Sci. Eng. Process Syst. Eng.* **2006**, *3*, 1735.

(8) Urey, H. C.; Rittenberg, D. *J. Chem. Phys.* **1933**, *1*, 137.

(9) Urey, H. C. *J. Chem. Soc.* **1947**, 562.

(10) Palko, A. A.; Begun, G. M.; Landau, L. *J. Chem. Phys.* **1962**, *37*, 552.

(11) Begun, G. M.; Palko, A. A. *J. Chem. Phys.* **1963**, *38*, 2112.

(12) Leung, F.-Y.; Colussi, A. J.; Hoffmann, M. R. *J. Phys. Chem. A* **2001**, *105*, 8073.

(13) Schauble, E. A.; Rossman, G. R.; Taylor, H. P. *Geochim. Cosmochim. Acta* **2003**, *67*, 3267.

(14) Schauble, E. A.; Rossman, G. R.; Taylor, H. P. *Geochim. Cosmochim. Acta* **2002**, *66*, A675.

(15) Schauble, E. A.; Rossman, G. R.; Taylor, H. P. *Geochim. Cosmochim. Acta* **2001**, *65*, 2487.

(16) Jarzecki, A. A.; Anbar, A. D.; Spiro, T. G. *J. Phys. Chem. A* **2004**, *108*, 2726.

(17) Weeks, C. L.; Anbar, A. D.; Wasylenki, L. E.; Spiro, T. G. *J. Phys. Chem. A* **2007**, *111*, 12434.

(18) Rustad, J. R.; Nelmes, S. L.; Jackson, V. E.; Dixon, D. A. *J. Phys. Chem. A* **2008**, *112*, 542.

(19) Liu, Y.; Tossell, J. A. *Geochim. Cosmochim. Acta* **2005**, *69*, 3995.

(20) Rustad, J. R.; Bylaska, E. J. *J. Am. Chem. Soc.* **2007**, *129*, 2222.

(21) Lin, T.; Zhang, W.; Wang, L. *J. Phys. Chem. A* **2008**, *112*, 13600.

(22) Scott, A. P.; Radom, L. *J. Phys. Chem.* **1996**, *100*, 16502.

(23) Rauhut, G.; Pulay, P. *J. Phys. Chem.* **1995**, *99*, 3093.

(24) Harris, N. J. *J. Phys. Chem.* **1995**, *99*, 14689.

(25) Irikura, K. K.; Johnson, R. D.; Kacker, R. N. *J. Phys. Chem. A* **2005**, *109*, 8430.

(26) Merrick, J. P.; Moran, D.; Radom, L. *J. Phys. Chem. A* **2007**, *111*, 11683.

(27) Vanderryn, J. *J. Chem. Phys.* **1959**, *30*, 331.

(28) Dows, D. A. *J. Chem. Phys.* **1959**, *31*, 1637.

(29) Nakane, R.; Oyama, T. *J. Chem. Phys.* **1966**, *70*, 1146.

(30) Balfour, W. J. *Spectrochim. Acta A* **1983**, *39*, 795.

(31) Gellini, C.; Moroni, L.; Muniz-Miranda, M. *J. Phys. Chem. A* **2002**, *106*, 10999.

(32) Eisenhardt, C. G.; Gemechu, A. S.; Baumgartel, H.; Chelli, R.; Cardini, G.; Califano, S. *Phys. Chem. Chem. Phys.* **2001**, *3*, 5358.

(33) Taillandier, E.; Taillandier, M. *C. R. Seances Acad. Sci., Ser. C* **1966**, *263*, 1265.

(34) Møller, C.; Plesset, M. S. *Phys. Rev.* **1934**, *46*, 618.

(35) Frisch, M. J.; Headgordon, M.; Pople, J. A. *Chem. Phys. Lett.* **1990**, *166*, 275.

(36) Miehlich, B.; Savin, A.; Stoll, H.; Preuss, H. *Chem. Phys. Lett.* **1989**, *157*, 200.

(37) Becke, A. D. *J. Chem. Phys.* **1993**, *98*, 5648.

(38) Becke, A. D. *Phys. Rev. A* **1998**, *38*, 3098.

(39) Lee, C.; Yang, W.; Parr, R. G. *Phys. Rev. B* **1998**, *37*, 785.

(40) Frisch, M. J.; Trucks, G. W.; Schlegel, H. N.; Scuseria, G. E.; Robb, M. A.; Cheeseman, J. R.; Montgomery, J. A., Jr.; Vreven, T.; Kudin, K. N.; Burant, J. C.; Millam, J. M.; Iyengar, S. S.; Tomasi, J.; Barone, V.; Mennucci, B.; Cossi, M.; Scalamni, G.; Rega, N.; Petersson, G. A.; Nakatsuji, H.; Hada, M.; Ehara, M.; Toyota, K.; Fukuda, R.; Hasegawa, J.; Ishida, M.; Nakajima, T.; Honda, Y.; Kitao, O.; Nakai, H.; Klene, M.; Li, X.; Knox, J. E.; Hratchian, H. P.; Cross, J. B.; Bakken, V.; Adamo, C.;

Jaramillo, J.; Gomperts, R.; Stramann, R. E.; Yazyev, O.; Austin, A. J.; Cammi, R.; Pomelli, C.; Ochterski, J. W.; Ayala, P. Y.; Morokuma, K.; Voth, G. A.; Salvador, P.; Dannenberg, J. J.; Zakrzewski, V. G.; Dapprich, S.; Daniels, A. D.; Strain, M. C.; Farkas, O.; Malick, D. K.; Rabuck, A. G.; Clifford, S.; Cioslowski, J.; Stefanov, B. B.; Liu, G.; Liashenko, A.; Piskorz, P.; Komaromi, I.; Martin, R. L.; Fox, D. J.; Keith, T.; Al-Laham, M. A.; Peng, C. Y.; Nanayakkara, A.; Challacombe, M.; Grill, P. M. W.; Johnson, B.; Chen, W.; Wong, M.,W.; Gonzalez, C.; Pople, J. A. *Gaussian 03*, Revision B.05; Gaussian, Inc.: Wallingford, CT, 2004.

(41) Gage, D. M.; Barker, E. F. *J. Chem. Phys.* **1939**, *7*, 455.

(42) Nielsen, A. H. *J. Chem. Phys.* **1954**, *22*, 659.

(43) Mckean, D. C. *Chem. Soc. Rev.* **1978**, *7*, 399.

(44) Johnson, C. M.; Skulan, J. L.; Beard, B. L.; Sun, H.; Nealson, K. H.; Braterman, P. S. *Earth Planet. Sci. Lett.* **2002**, *195*, 141.

(45) Welch, S. A.; Beard, B. L.; Johnson, C. M.; Braterman, P. S. *Geochim. Cosmochim. Acta* **2003**, *67*, 4231.

JP810328R